Chromosome engineering to restore euploidy in cells harboring a complex rearrangement of chromosome 8

Sophia N. Lee[1], Lu Qiao[1], Sarah L. Thompson[1], Ryan A. Hagenson[1], Teresa Davoli[2], Jason M. Sheltzer[1†]

1. Yale University School of Medicine, New Haven, CT, USA.
2. Institute for Systems Genetics and Department of Biochemistry and Molecular Pharmacology, NYU Langone Health, New York, NY, USA.

† Corresponding author. Email: jason.sheltzer@yale.edu

Abstract

Chromosomal rearrangements on the short arm of chromosome 8 cause 8p syndrome, a rare developmental disorder characterized by neurodevelopmental delays, epilepsy, and cardiac abnormalities. While significant progress has been made in managing the symptoms of 8p syndrome and other conditions caused by large-scale chromosomal aneuploidies, no therapeutic approach has yet been demonstrated to target the underlying disease-causing chromosome. Here, we establish a two-step approach to eliminate the abnormal copy of chromosome 8 and restore euploidy in cells derived from an individual with a complex rearrangement of chromosome 8p. Transcriptomic analysis revealed 361 differentially expressed genes between the proband and the euploid revertant, highlighting genes both within and outside the 8p region that may contribute to 8p syndrome pathology. Our work demonstrates the feasibility of using chromosome engineering to correct complex aneuploidies in vitro and suggests a potential therapeutic avenue for disorders caused by chromosomal rearrangements.

Introduction

Large-scale gene copy number alterations are the most common cause of miscarriage and developmental disability in humans[1]. Disorders like Down syndrome, caused by the triplication of chromosome 21, and Cri du chat syndrome, caused by the deletion of a region of chromosome 5p, affect the expression of hundreds of genes and perturb normal development. 8p syndrome, caused by rearrangements affecting the p arm of chromosome 8, represents a rare class of developmental disorders and impacts about 1 in 10,000-30,000 live births a year[2].

Several different types of 8p rearrangements have been documented in the medical literature. The most common alteration affecting this region consists of a terminal distal deletion and an inverted duplication proximal to the chromosome 8 centromere, termed invdupdel(8p)[3]. This rearrangement arises from aberrant pairing and recombination events during meiosis, which may be due to the presence of the ß-defensin repeats and olfactory gene receptor clusters found within this region[4]. Individuals affected by 8p syndrome present with a variety of clinical phenotypes, including agenesis of the corpus callosum, epilepsy, and other neurodevelopmental delays[5].

Over the past several decades, the medical management of individuals with copy number disorders like Down syndrome has improved remarkably[6,7]. Aggressive and early interventions designed to address drivers of morbidity in these populations have resulted in the average lifespan of an individual with Down syndrome increasing from 25 years in 1983 to around 60 years in 2010[8]. However, to date, the successful treatment of individuals with copy number disorders has relied almost entirely on symptom management. Therapies designed to address the underlying genetic disorder, for instance, by inhibiting the function of a dosage-sensitive protein encoded in a triplicated region, have not proven to be successful[9]. The failure of targeted therapies to produce clinical benefit raises the possibility that other interventions may best be able to correct the underlying genetic pathology.

An alternate approach to treat disorders caused by large-scale chromosomal abnormalities would be to directly manipulate the causative chromosome(s). For these techniques, broadly called “chromosome therapies”, the disease-causing chromosome may be silenced, eliminated, or replaced with a non-pathological copy[10,11,12]. Pioneering work conducted in iPS cells derived from individuals with Down syndrome demonstrated that the extra copy of chromosome 21 could be silenced through the use of the XIST noncoding RNA or removed through the introduction of a genetic negative selection cassette[10,13]. Further research revealed that the generation and passaging of iPS cells themselves could promote reversion to a euploid state, likely because of the detrimental fitness effects of the initial aneuploidy[14,15]. “Chromosome therapy” may be particularly appealing for addressing a complex disorder like 8p syndrome, as no individual dosage-sensitive gene within this region has been demonstrated to drive pathological development, and individuals with this disorder exhibit significant variability in the size and location of the chromosomal rearrangements [2,5,16.]

A number of technical hurdles remain for implementing chromosome therapy as a medical intervention[10]. However, while this approach has not yet been successfully translated into the clinic, chromosome therapy can be utilized to generate a variety of powerful research tools. In particular, chromosome therapy can be applied to create matched cells that have or lack a specific chromosome abnormality but are otherwise genetically identical. Such cell line pairs bypass the confounding effects of genetic variability that complicate comparisons between cells derived from an individual with a chromosomal abnormality and their unaffected siblings or parents. Isogenic cell pairs can be ideal tools for drug screens, gene expression analysis, and investigations into the biological consequences of a specific chromosome rearrangement.

To date, successful examples of chromosome therapy applied *in vitro* have been limited to trisomies and ring chromosomes[13,15,17,18,19,20]. To our knowledge, the elimination of a complex rearrangement like invdupdel(8p) has not been reported. Here, we leveraged cutting-edge chromosome engineering techniques to derive a euploid revertant cell line from iPS cells established from an individual with invdupdel(8p).

Results

Whole-genome sequencing of invdupdel(8p) iPS cells

8p syndrome is characterized by a wide spectrum of clinical phenotypes, including neurological, visual, and musculoskeletal abnormalities (Figure 1A). We received a line of iPS cells with invdupdel(8p) from Project 8p, a philanthropic group dedicated to improving the care of individuals affected by 8p syndrome. We performed low pass whole-genome sequencing to determine the extent of the copy number alterations exhibited by the proband. The deletion spanned from the telomere of chromosome 8p to position 7,247,573 and encompassed 23 protein-coding genes, while the duplication spanned from position 11,828,865 – 40,361,770 and encompassed 172 protein-coding genes (Figure 1B-C)[21,22,23]. No other aneuploidies were detected in the proband.

Prolonged passaging of invdupdel(8p) iPS cells fails to restore euploidy

Previous reports in the literature have demonstrated that the prolonged growth of aneuploid iPS cells in culture can sometimes result in the isolation of derivative cells with euploid karyotypes[14,20]. This may be because most aneuploidies confer a fitness disadvantage in primary cells, and rare euploid cells arising from chromosome missegregation events are able to outcompete the aneuploid starting population and overtake the culture[24,25]. We therefore sought to determine whether we could isolate invdupdel(8p) revertants with a euploid karyotype through continuous passaging (Figure 2A). We grew the proband's cells for approximately 130 days in culture, until passage 50. We then designed a TaqMan-based strategy to assess the copy number of the invdupdel(8p) region (Figure 2B)[26]. qPCR confirmed the presence of two copies of the proband-deleted region and two copies of the proband-duplicated region in iPS cells derived from the proband's parents (Figure 2C). We performed qPCR on the proband cell line at five timepoints spanning from passage 12 to passage 50, but we did not detect any evidence for the emergence of a euploid population (Figure 2C). We conclude that prolonged passaging is insufficient to restore euploidy in this proband's invdupdel(8p) iPS cells.

Inducing missegregation to generate iPS cells with trisomy 8

We noted that previous reports describing the successful isolation of euploid revertants from aneuploid iPS cell lines were primarily obtained from trisomic starting populations, in which a single chromosome missegregation event generated cells with the desired disomic karyotype. In contrast, isolation of euploid revertants from invdupdel(8p) cells would require both the loss of the chromosome harboring the rearrangement and duplication of the remaining homologue. We therefore hypothesized that two possible factors could explain our failure to isolate spontaneous revertants from invdupdel(8p) iPS cells. First, the rate of chromosome missegregation in this iPS cell line may not have been sufficient to produce the two missegregation events necessary to restore euploidy. Alternately, monosomies are very poorly tolerated by primary cells, and even transient loss of the rearranged copy of 8p may have been incompatible with cellular viability[27,28,29].

To circumvent these challenges, we developed an alternate approach to facilitate the isolation of invdupdel(8p) revertant cells. We treated the proband cells with a sublethal dose of the Mps1 inhibitor AZ3146, which we and others have shown ablates the mitotic checkpoint and enhances the rate of chromosome missegregation.[30,31,32,33] We hypothesized that transient exposure to AZ3146 could have two potential benefits: first, by increasing the frequency of chromosome missegregation, we could have a greater likelihood of isolating cells that spontaneously acquired a euploid karyotype. Alternately, treatment with AZ3146 could lead to the incidental production of cells trisomic for chromosome 8, which could then serve as a stable intermediate for the subsequent isolation of a euploid revertant cell line (Figure 3A).

Following treatment with AZ3146, we isolated 52 viable iPS clones. TaqMan qPCR using 8p-specific probes did not reveal any clones with a euploid karyotype. However, we identified two clones that appeared to have acquired a trisomy of chromosome 8 (Figure 3B and S1). We performed low pass whole-genome sequencing on these clones and we established that they harbored a trisomy of chromosome 8q, a tetrasomy of the duplicated region of chromosome 8p, and a disomy of the 8p-deleted region. Clone 33 also exhibited a partial gain of chromosome 19, while no other aneuploidies were apparent in clone 31 (Figure 3C). We therefore chose clone 31 to use in our subsequent efforts to restore chromosome 8 euploidy.

Inducing targeted missegregation to generate a euploid revertant iPS cell line

Simultaneous to our efforts to accelerate chromosome missegregation with an Mps1 inhibitor, Davoli and colleagues published a new system for targeted chromosome missegregation[34]. In this approach, called KaryoCreate, catalytically-inactive dCas9 is used to target a checkpoint-deficient kinetochore protein to a specific mammalian centromere (Figure 4A). The mutant kinetochore protein prevents correct amphitelic biorientation, leading to the missegregation of the targeted chromosome. We therefore sought to apply the KaryoCreate system to restore euploidy in our invdupdel(8p) iPS cell lines. We elected to conduct these experiments using clone 31, which harbors a trisomy of chromosome 8, as inducing loss of the rearranged copy of chromosome 8 would be sufficient to restore euploidy in this clone.

We transiently transfected clone 31 with plasmids encoding the dCas9 fusion protein and a gRNA specific to the chromosome 8 centromere. We then isolated 43 viable clones and screened them via TaqMan to assess the copy number of chromosome 8. qPCR analysis identified one clone that appeared to have lost the chromosome 8 trisomy (Figure 4B and S2A). To rule out the possibility that this clone resulted from cell culture contamination, we performed STR profiling on iPS cells from the two parents, the proband, and the apparent revertant. This analysis confirmed that the revertant clone was derived from the proband, and analysis of the D8S1179 marker on chromosome 8 revealed that it harbored an isodisomy for a paternal copy of chromosome 8 (Figure S2B). Finally, we performed low pass whole-genome sequencing on the revertant which confirmed the loss of the rearranged chromosome and the restoration of a euploid karyotype (Figure 4C).

Gene expression analysis in proband and revertant iPS cells

To improve our understanding of how invdupdel(8p) affects normal development, we performed RNAseq on iPS cells derived from the proband, the two parents, and on the revertant clone. We first compared gene expression on chromosome 8 between the proband and the revertant (Figure 5A). In the region corresponding to the deletion, genes in the proband were expressed on average 43% lower, and in the region corresponding to the duplication, genes in the proband were expressed on average 56% higher, relative to the revertant. These results indicate that the 8p rearrangement results in transcriptional alterations that are broadly proportional to the change in DNA copy number.

We hypothesized that the isolation of a genetically-matched euploid revertant would allow us to precisely identify genes and processes dysregulated by the 8p rearrangement. In contrast, comparisons between the proband and the parents may be confounded both by genetic differences and by differences that arose during the cellular reprogramming process. We therefore performed genome-wide differential expression analysis between either the proband and the revertant or between the proband and the parents. Consistent with our hypothesis, we found that 1,401 genes were differentially expressed between the proband and the parents, and only 361 genes were differentially expressed between the proband and the revertant (Figure 5B). We speculate that these 361 genes are highly enriched for the genes that contribute to invdupdel(8p) pathology (Table S1).

Within the deleted region, we observed that CLN8 and MCPH1 were significantly downregulated (Figure 5C). Mutations in CLN8 have been reported to cause epilepsy and neurodegeneration[35]. Mutations in MCPH1 have been associated with microcephaly[36]. Within the duplicated region, genes like RHOBTB2 and UNC5D were significantly overexpressed. RHOBTB2 has been identified in prior studies as a potential candidate 8p driver gene due to its association with epileptic encephalopathy and other phenotypes overlapping with 8p syndrome[16]. UNC5D overexpression has been associated with delayed migration of radial cortical neurons[37]. Finally, we observed that a majority of differentially expressed genes were located outside of chromosome 8p. Notable genes included NAV3, which was downregulated, and CNTN4, which was upregulated. Prior studies have linked NAV3 to processes like neuronal cell migration; impairment in this process can contribute to agenesis of the corpus callosum and hypotonia[38]. CNTN4 encodes a neuronal membrane protein that has roles in the plasticity and maintenance of neuronal networks. Duplications in CNTN4 have been observed in cohorts of individuals with autism spectrum disorder[39,40].

Finally, we conducted gene set enrichment analysis, comparing the proband and the revertant. We observed that certain fundamental biological processes, including protein translation and DNA methylation, were

downregulated in the proband (Figure 5D and Table S2). Additionally, pathways related to neurodevelopment, including neural cell migration and hindbrain development, were enriched among downregulated genes. Fewer pathways were upregulated in the proband; the most significantly-upregulated process was homophilic cell adhesion (Table S2). Further analysis of gene expression and cellular differentiation in these iPS lines may shed additional light on how 8p rearrangements perturb normal developmental processes.

Discussion

Here, we report the first successful isolation of a euploid clone derived from an individual with a complex chromosomal rearrangement. We achieved this through a two-step process, in which we established an intermediate cell population harboring a trisomy of the affected chromosome and then induced the loss of a single copy of the rearranged homologue. Prior work has demonstrated that prolonged passaging can be sufficient to restore euploidy in trisomic iPS cells; however, we did not observe spontaneous revertants from our invdupdel(8p) starting population. Whole chromosome aneuploidies induce a significant fitness cost in primary cells[41] and we speculate that the effects of invdupdel(8p) on iPS cell proliferation were not sufficient to allow the isolation of a spontaneous revertant population.

Instead, we used transient treatment with an Mps1 inhibitor to isolate a clone harboring a trisomy of chromosome 8, and then we applied KaryoCreate to promote the missegregation of chromosome 8 and facilitate the isolation of a euploid revertant[34]. KaryoCreate is one of several new strategies for targeted chromosome engineering that have recently been developed. Other methods include ReDACT, in which CRISPR is used to introduce a positive-negative selection cassette onto an aneuploid chromosome, and a kinesin-based approach in which a plant kinesin is used to drag a chromosome to the wrong centrosome[42,43,44]. We elected to use KaryoCreate, as we anticipated that it would produce less DNA damage than these other methods and because it does not require stable modification of the target cell's genome. Our work verifies the earlier publication from the Davoli lab and suggests that KaryoCreate can be an effective strategy for inducing chromosome-specific missegregation events.

Gene expression analysis performed across the proband, parental, and revertant iPS cells revealed many fewer differentially-expressed genes when the proband and the revertant were directly compared. We speculate that this is because the proband and the revertant are isogenic while the proband and each parent share only 50% genetic similarity. Our expression analysis revealed 361 genes that were differentially expressed between the proband and the revertant. Notably, more than 300 of these genes were located outside the invdupdel(8p) region, highlighting how this chromosomal rearrangement can impact the transcriptional landscape throughout the genome. In future work, these matched cell pairs could represent ideal tools for multiple follow-up investigations, including phenotypic assays to uncover how the 8p rearrangement affects cellular physiology and drug screens to identify compounds capable of rescuing invdupdel(8p)-induced defects.

Finally, chromosome engineering represents a powerful potential approach for treating multiple disorders caused by chromosomal rearrangements and copy number changes. Prior investigators have silenced or eliminated simple trisomies and chromosomal duplications in tissue culture through single genetic manipulations[13,18,45]. To our knowledge, the work described in this manuscript represents the first instance in which a complex chromosome rearrangement has been genetically eliminated from human cells. However, we were only able to achieve this correction via a two-step process that included a trisomic intermediate. The currently-laborious nature of our protocol represents an important hurdle for successful clinical translation. In future work, the establishment of improved techniques for chromosome engineering may facilitate the development of therapeutic strategies to treat 8p syndrome and other aneuploidy-associated disorders using chromosome therapy.

Methods

Acquisition of biological specimens

iPS cells from an individual with invdupdel(8p) as well as two parental iPS cell lines were provided by Project 8p[46]. Cell lines were received at passage 13. STR profiling was performed at the University of Arizona Genetics

Core facility and verified the relationship between parental and proband cell lines. Research was conducted in accordance with Yale University and NIH guidelines (IRB Protocol ID: 2000033853).

Cell culture conditions

iPS cells were cultured in mTeSR Plus (STEMCELL Technologies, cat. no. 100-0276), on plates coated in Matrigel (Corning, cat. no. 356231). Routine colony passaging and dissociation were done using Dispase (STEMCELL Technologies, cat. no. 07913). Media was changed daily, and cells were passaged every 4 days. For single cell applications, cells were dissociated using Accutase (STEMCELL Technologies, cat. no. 07920) and plated on Matrigel coated plates containing mTeSR Plus supplemented with 10 μM Y-27632 (STEMCELL Technologies, cat. no. 72304). Cells were maintained at 5% CO_2, 5% O_2, 37° C in a humidified chamber.

TaqMan copy number analysis

Genomic DNA from iPS cells was extracted using Qiagen DNeasy Blood & Tissue Kit (cat. no. 69506). Each sample was loaded in quadruplicate in 384 well plates. Quantitative PCR was performed using TaqPath ProAmp Master Mix (Applied Biosystems, cat. no. A30867). A probe targeting RNaseP (Applied Biosystems, cat. no. 4316831) was used as a reference assay. Other TaqMan copy number probes from Applied Biosystems that were used in this work include: MICU3 (Assay ID: Hs06219542_cn, location: Chr.8:17109660), CSMD1 (Assay ID: Hs06164679_cn, location: Chr.8:2944759), and CRISPLD1 (Assay ID: Hs02746949_cn, location: Chr.8:75032222).

Genomic copy number was typically calculated by normalizing to MCF10A, a human mammary epithelial cell line with a near-diploid karyotype[42]. For the analysis in Figure 4B, CRISPLD1 was normalized to the proband rather than to MCF10A.

Cloning of mCherry into KNL1^{Mut}-dCas9 KaryoCreate Plasmid

To facilitate the isolation of iPS cells transiently transfected with the KaryoCreate system, we introduced a fluorescent vector into the KNL1^{Mut}-dCas9 plasmid. The blasticidin resistance marker in pHAGE-KNL1^{Mut}-dCas9 was replaced with the mCherry construct from LRCherry2.1 (Addgene #108099) via HiFi assembly (New England Biolabs, cat. no. E2621L), using PCR primers atagctaggtagcctagagggcccgcggttACTTTGGCGCCGGCT and atattcatttctttgcaagttaCTGAATAATAAGATGACATGAACTACTATACGTACTGC to generate the mCherry-KNL1^{Mut}-dCas9 plasmid (Addgene: 229940). The plasmid sequence was verified using whole-plasmid sequencing (Plasmidsaurus).

Generation of trisomic proband intermediate cells

Transient chromosome missegregation was induced via treatment with the Mps1 inhibitor AZ3146 (Selleck Chemicals, cat. no. S2731). Based on prior experiments testing the effects of AZ3146 treatment,[31,47] we elected to use 1.5 μM AZ3146. 2 million cells were treated with AZ3146 for 48 hours, and then the drug was washed out. 24 hours after drug washout, the cells were harvested and single-cell sorted. 8p copy number was determined via qPCR in approximately 60 clones, and two clones that harbored a trisomy of chromosome 8 were identified and retained for further characterization.

Generation of a revertant iPS cell line

Approximately 1 x 10^6 trisomic proband iPS cells were transiently co-transfected with a plasmid that expressed a gRNA (Addgene: 229941) specific to the chromosome 8 centromere region and the mCherry-KNL1^{Mut}-dCas9 plasmid. Proband cells were transfected using the Amaxa 4D-Nucleofector X (Lonza) system. After nucleofection, the buffer mixture containing cells was seeded onto two wells of a Matrigel-coated six-well dish.

8p copy number was determined via qPCR in approximately 100 clones, and one clone in which disomy of chromosome 8 had been restored was retained for further characterization.

RNA-seq

Total cellular RNA was isolated using the Qiagen RNeasy Mini Kit (Qiagen, cat. no. 74106) and submitted to Novogene for RNA-seq and quantification. Raw data in FASTQ format were processed using Novogene's analysis pipeline to generate raw read counts. Read counts were filtered to remove lowly expressed genes and normalized across samples using TMM normalization with edgeR (v4.2.1)[48]. Differential expression analysis was performed with edgeR (v4.2.1). Samples extracted from the mother's iPS cells and the father's iPS cells were combined into a group labeled "Parents". For the analysis in Figure 5B, an additional threshold of absolute log2 fold change > 1 was applied to identify differentially expressed (DE) genes between the proband and parents, as well as between the proband and the revertant.

CPM counts were calculated and transformed to a log2 scale using edgeR (v4.2.1) and ranked using the Signal2Noise metric with the local version of the GSEA tool (v4.3.3) http://www.broadinstitute.org/gsea/index.jsp. Gene Set Enrichment Analysis (GSEA) was performed using the Hallmark, C2, and C5 gene sets from MSigDB, with clusterProfiler (v4.12.6)[49,50]. Statistical testing was performed using a two-tailed Pearson's Chi-Square test. Analyses were performed using R Statistical Software (v4.4.1; R Core Team 2024) and tidyverse (v2.0.0)[51,52,53,54,55]. Gene expression data is available at GSE281425.

Whole genome sequencing and copy number alteration detection

Genomic DNA was isolated as described above. Sequencing was performed using Short-Read Human WGS services provided by GENEWIZ from Azenta Life Sciences, as described (https://www.genewiz.com). After sequencing, copy number alterations in the samples were inferred by a custom Nextflow wrapper (v1.0) for CNVKit (v0.9.11) with "batch --method wgs" command, specifying a bin size of 100,000[56,57,58]. For selected samples, a bin size of 50,000 was used to improve segmentation sensitivity and copy number estimation. Absolute copy numbers of segments were inferred by CNVkit with "call" command, while copy numbers of the bins were derived from log2 copy ratios. Plots of copy number alterations were generated using a custom Python script (v3.12.4) with matplotlib (v3.8.4) and pandas (v2.2.2)[59,60,61]. The script was adapted from CNVkit's scatter.py with specific modifications to enhance visual representation. The full details of the modifications, as well as the complete workflow, are available in a public repository on GitHub https://github.com/sheltzer-lab/Karyotyping.

Data Visualization

Scientific illustrations were assembled using BioRender. Graphs were generated using GraphPad Prism. GSEA plots were generated using enrichplot (v1.24.4)[62]. Figure 5B was created using ggplot2 (v3.5.1), with ggthemes (v5.1.0) and MetBrewer (v0.2.0) used for artistic purposes[63,64,65].

Acknowledgements

We are grateful to Project 8p and to the anonymous donors who provided the biological specimens used in this analysis. This work was supported in part by a research grant from Project 8p. Research in the Sheltzer Lab is supported by NIH grants R01CA237652 and R01CA276666, Department of Defense grant W81XWH-20-1-068, an American Cancer Society Research Scholar Grant, and a sponsored research agreement from Ono Pharmaceuticals. We thank members of the Yale hESC/iPSC Core Facility, for providing reagents and assistance with iPS cell culture. Additionally, we thank the Yale Flow Cytometry Core for their assistance with cell sorting. The Core is supported in part by an NCI Cancer Center Support Grant # NIH P30 CA016359. The BD Symphony was funded by shared instrument grant # NIH S10 OD026996. Work in the Davoli Lab is supported by NIH grant R37CA248631.

Declaration of interests

J.M.S. has received consulting fees from Merck, Pfizer, Ono Pharmaceuticals, and Highside Capital Management, is a member of the advisory boards of Tyra Biosciences, BioIO, and the Chemical Probes Portal, and is a co-founder of Meliora Therapeutics. J.M.S. and S.L.T. are co-inventors on a patent related to chromosome engineering. T.D. has filed a patent on the KaryoCreate technology.

Figure Legends

Figure 1: Karyotype of the invdupdel(8p) proband iPS line

A. Schematic listing commonly observed symptoms in individuals affected by invdupdel(8p).

B. Diagram delineating altered regions in the proband. The deleted region is marked in blue. The region that is inverted and duplicated is marked in red.

C. Karyotype of the invdupdel(8p) proband iPS line. The deleted region is highlighted in blue. The region that is inverted and duplicated is marked in red.

Figure 2: Prolonged passaging fails to induce spontaneous loss of the invdupdel(8p) rearrangement

A. Schematic detailing the prolonged passaging of proband cells to induce spontaneous loss of the rearranged copy of chromosome 8.

B. Generation of copy number Taqman probes specific to genes contained within the invdupdel(8p) altered regions. CSMD1 is a gene located within the deleted region, and MICU3 is a gene located within the duplicated region.

C. Copy numbers of CSMD1 and MICU3 after passaging proband cells for 12, 22, 33, 40, and 50 passages. Mean ± SEM, data from representative trials are shown ($n \geq 3$ total trials). Genomic DNA from the near-diploid MCF10A cell line was used as a control.

Figure 3: Generation of a chromosome 8 trisomy through Mps1 inhibition

A. Schematic describing two possible ways by which euploidy could be restored in proband cells after treatment with AZ3146. One method consists of the loss of the rearranged copy of chromosome 8 coupled with the duplication of the remaining chromosome. The second method consists of gaining an unrearranged copy of chromosome 8 and then subsequently losing the rearranged homologue.

B. Copy numbers of CSMD1 and MICU3 in proband clones treated with AZ3146. Trisomic clones 31 and 33 are labeled with stars. Mean ± SEM, data from representative trials are shown ($n \geq 3$ total trials). Genomic DNA from MCF10A cells was used as a diploid control.

C. Karyotypes of two clones that have gained an additional unrearranged copy of chromosome 8 following AZ3146 treatment.

Figure 4: Restoration of euploidy using the KaryoCreate system

A. Schematic describing the use of the KaryoCreate system to induce the missegregation of a specific chromosome.

B. Copy numbers of CSMD1, MICU3, and CRISPLD1 (a gene located on the q arm of chromosome 8), in trisomic proband clones that were transiently transfected with KaryoCreate plasmids. Mean ± SEM, data from representative trials are shown ($n \geq 3$ total trials). Genomic DNA extracted from MCF10A cells was used as a diploid control.

C. Karyotype of the euploid revertant clone 31.3.

Figure 5: Comparing gene expression between proband and revertant iPS cells

A. Diagram comparing relative gene expression vs chromosome position along chromosome 8. The deleted region is highlighted in blue, the duplicated region is highlighted in red, and the position of the centromere is highlighted in gray.

B. Bar graph displaying the number of differentially expressed genes according to the chromosomal region. Statistical testing was performed via Chi-squared test. ns, $p \geq 0.05$; *, $p \leq 0.05$; **, $p \leq 0.01$; ***, $p \leq 0.001$.

C. Representative genes that were identified as differentially expressed between the proband and revertant iPS lines. A complete list of differentially expressed genes is included in Table S1.

D. Representative biological pathways enriched among genes that were downregulated in the proband relative to the revertant. A complete list of GSEA results is included in Table S2.

Supplemental Figure Legends

Figure S1: Copy number analysis of proband clones after treatment with AZ3146

Copy numbers of CSMD1 and MICU3 in clones treated with AZ3146. Trisomic clones 31 and 33 are labeled with stars. Mean ± SEM, data from representative trials are shown ($n \geq 3$ total trials).

Figure S2: Analysis of trisomic clones transfected with KaryoCreate plasmids

A. Copy numbers of CSMD1 and MICU3 in trisomic clones after transient transfection with KaryoCreate plasmids. Revertant clone 31.3 is labeled with a star. Mean ± SEM, data from representative trials are shown ($n \geq 3$ total trials). Genomic DNA extracted from MCF10A cells was used as a diploid control.

B. STR analysis of the parental, proband, and revertant cells. The D8S1179 locus, which is located on chromosome 8, is highlighted in yellow.

Works Cited

1. Sheltzer, J. M. & Amon, A. The aneuploidy paradox: costs and benefits of an incorrect karyotype. *Trends in Genetics* **27**, 446–453 (2011).
2. Lo Bianco, M. *et al.* Deciphering the Invdupdel(8p) Genotype-Phenotype Correlation: Our Opinion. *Brain Sci* **10**, 451 (2020).
3. Santucci, K. *et al.* Chromosome 8p Syndromes Clinical Presentation and Management Guidelines. *Clinical Genetics* **n/a**, (2024).
4. Giglio, S. *et al.* Olfactory receptor-gene clusters, genomic-inversion polymorphisms, and common chromosome rearrangements. *Am J Hum Genet* **68**, 874–883 (2001).
5. Vibert, R. *et al.* Neurodevelopmental phenotype in 36 new patients with 8p inverted duplication-deletion: Genotype-phenotype correlation for anomalies of the corpus callosum. *Clin Genet* **101**, 307–316 (2022).
6. Hendrix, J. A. *et al.* Opportunities, barriers, and recommendations in down syndrome research. *Translational science of rare diseases* **5**, 99 (2021).
7. Skotko, B. G., Davidson, E. J. & Weintraub, G. S. Contributions of a specialty clinic for children and adolescents with Down syndrome. *American Journal of Medical Genetics Part A* **161**, 430–437 (2013).
8. Glasson, E. J., Jacques, A., Wong, K., Bourke, J. & Leonard, H. Improved Survival in Down Syndrome over the Last 60 Years and the Impact of Perinatal Factors in Recent Decades. *The Journal of Pediatrics* **169**, 214-220.e1 (2016).
9. Jiang, J. *et al.* Translating Dosage Compensation to Trisomy 21. *Nature* **500**, 296 (2013).
10. Gupta, K., Czerminski, J. T. & Lawrence, J. B. Trisomy silencing by XIST: translational prospects and challenges. *Human Genetics* **143**, 843 (2024).
11. Zuo, E. *et al.* CRISPR/Cas9-mediated targeted chromosome elimination. *Genome Biology* **18**, 224 (2017).
12. Paulis, M. *et al.* Chromosome transplantation as a novel approach for correcting complex genomic disorders. *Oncotarget* **6**, 35218 (2015).
13. Li, L. B. *et al.* Trisomy correction in Down syndrome induced pluripotent stem cells. *Cell Stem Cell* **11**, 615–619 (2012).
14. Ya, A., Deng, C. & Godek, K. M. Cell Competition Eliminates Aneuploid Human Pluripotent Stem Cells. *bioRxiv* 2024.05.08.593217 (2024) doi:10.1101/2024.05.08.593217.

15. Akutsu, S. N. *et al.* iPSC reprogramming-mediated aneuploidy correction in autosomal trisomy syndromes. *PLOS ONE* **17**, e0264965 (2022).
16. Okur, V. *et al.* Clinical and genomic characterization of 8p cytogenomic disorders. *Genet Med* **23**, 2342–2351 (2021).
17. Li, T. *et al.* The spontaneous differentiation and chromosome loss in iPSCs of human trisomy 18 syndrome. *Cell Death & Disease* **8**, e3149 (2017).
18. Inoue, M. *et al.* Autonomous trisomic rescue of Down syndrome cells. *Lab Invest* **99**, 885–897 (2019).
19. Hirota, T. *et al.* Fertile offspring from sterile sex chromosome trisomic mice. *Science* **357**, 932–935 (2017).
20. Bershteyn, M. *et al.* Cell-autonomous correction of ring chromosomes in human induced pluripotent stem cells. *Nature* **507**, 99–103 (2014).
21. Durinck, S. *et al.* BioMart and Bioconductor: a powerful link between biological databases and microarray data analysis. *Bioinformatics* **21**, 3439–3440 (2005).
22. Durinck, S., Spellman, P. T., Birney, E. & Huber, W. Mapping identifiers for the integration of genomic datasets with the R/Bioconductor package biomaRt. *Nat Protoc* **4**, 1184–1191 (2009).
23. Harrison, P. W. *et al.* Ensembl 2024. *Nucleic Acids Research* **52**, D891–D899 (2024).
24. Thompson, S. L. & Compton, D. A. Proliferation of aneuploid human cells is limited by a p53-dependent mechanism. *J Cell Biol* **188**, 369–381 (2010).
25. Vasudevan, A. *et al.* Aneuploidy as a promoter and suppressor of malignant growth. *Nat Rev Cancer* **21**, 89–103 (2021).
26. Mayo, P. *et al.* CNV analysis using TaqMan copy number assays. *Curr Protoc Hum Genet* **Chapter 2**, Unit2.13 (2010).
27. Magnuson, T. *et al.* The early lethality of autosomal monosomy in the mouse. *J Exp Zool* **236**, 353–360 (1985).
28. Chunduri, N. K. *et al.* Systems approaches identify the consequences of monosomy in somatic human cells. *Nature Communications* **12**, 5576 (2021).
29. Biancotti, J. C. *et al.* The in vitro survival of human monosomies and trisomies as embryonic stem cells. *Stem Cell Res* **9**, 218–224 (2012).

30. Hewitt, L. *et al.* Sustained Mps1 activity is required in mitosis to recruit O-Mad2 to the Mad1–C-Mad2 core complex. *J Cell Biol* **190**, 25–34 (2010).
31. Vasudevan, A. *et al.* Single-Chromosomal Gains Can Function as Metastasis Suppressors and Promoters in Colon Cancer. *Dev Cell* **52**, 413-428.e6 (2020).
32. Santaguida, S., Tighe, A., D'Alise, A. M., Taylor, S. S. & Musacchio, A. Dissecting the role of MPS1 in chromosome biorientation and the spindle checkpoint through the small molecule inhibitor reversine. *Journal of Cell Biology* **190**, 73–87 (2010).
33. Kwiatkowski, N. *et al.* Small-molecule kinase inhibitors provide insight into Mps1 cell cycle function. *Nature Chemical Biology* **6**, 359–368 (2010).
34. Bosco, N. *et al.* KaryoCreate: A CRISPR-based technology to study chromosome-specific aneuploidy by targeting human centromeres. *Cell* **186**, 1985-2001.e19 (2023).
35. Sharkia, R. *et al.* CLN8 Gene Compound Heterozygous Variants: A New Case and Protein Bioinformatics Analyses. *Genes* **13**, 1393 (2022).
36. Kristofova, M., Ori, A. & Wang, Z.-Q. Multifaceted Microcephaly-Related Gene MCPH1. *Cells* **11**, 275 (2022).
37. Seiradake, E. *et al.* FLRT Structure: Balancing Repulsion and Cell Adhesion in Cortical and Vascular Development. *Neuron* **84**, 370–385 (2014).
38. Ghaffar, A. *et al.* Variants of NAV3, a neuronal morphogenesis protein, cause intellectual disability, developmental delay, and microcephaly. *Communications Biology* **7**, 831 (2024).
39. Glessner, J. T. *et al.* Autism genome-wide copy number variation reveals ubiquitin and neuronal genes. *Nature* **459**, 569–573 (2009).
40. Zhang, S. Q. *et al.* Intragenic *CNTN4* copy number variants associated with a spectrum of neurobehavioral phenotypes. *European Journal of Medical Genetics* **63**, 103736 (2020).
41. Williams, B. R. *et al.* Aneuploidy affects proliferation and spontaneous immortalization in mammalian cells. *Science* **322**, 703–709 (2008).
42. Girish, V. *et al.* Oncogene-like addiction to aneuploidy in human cancers. *Science* **381**, eadg4521 (2023).
43. Truong, M. A. *et al.* A kinesin-based approach for inducing chromosome-specific mis-segregation in human cells. *The EMBO Journal* **42**, e111559 (2023).

44. Tovini, L. *et al.* Targeted assembly of ectopic kinetochores to induce chromosome-specific segmental aneuploidies. *EMBO J* **42**, e111587 (2023).

45. Munezane, H. *et al.* Elimination of the extra chromosome of Dup15q syndrome iPSCs for cellular and molecular investigation. *European Journal of Cell Biology* **103**, 151446 (2024).

46. Home. *Project8p* https://project8p.org/.

47. Lukow, D. A. *et al.* Chromosomal instability accelerates the evolution of resistance to anti-cancer therapies. *Developmental Cell* **56**, 2427-2439.e4 (2021).

48. Chen, Y., Chen, L., Lun, A. T. L., Baldoni, P. L. & Smyth, G. K. edgeR 4.0: powerful differential analysis of sequencing data with expanded functionality and improved support for small counts and larger datasets. 2024.01.21.576131 Preprint at https://doi.org/10.1101/2024.01.21.576131 (2024).

49. Carlson, M. _org.Hs.eg.db: Genome wide annotation for Human_. R package. (2024).

50. Xu, S. *et al.* Using clusterProfiler to characterize multiomics data. *Nat Protoc* 1–29 (2024) doi:10.1038/s41596-024-01020-z.

51. R Core Team. R: A Language and Environment for Statistical Computing. R Foundation for Statistical Computing (2024).

52. Wickham, H. *et al.* Welcome to the Tidyverse. *Journal of Open Source Software* **4**, 1686 (2019).

53. Wickham, H. *et al.* readxl: Read Excel Files. (2023).

54. Wickham, H. *et al.* dplyr: A Grammar of Data Manipulation. (2023).

55. Wickham, H. *et al.* tidyr: Tidy Messy Data. (2024).

56. Talevich, E., Shain, A. H., Botton, T. & Bastian, B. C. CNVkit: Genome-Wide Copy Number Detection and Visualization from Targeted DNA Sequencing. *PLOS Computational Biology* **12**, e1004873 (2016).

57. Venkatraman, E. S. & Olshen, A. B. A faster circular binary segmentation algorithm for the analysis of array CGH data. *Bioinformatics* **23**, 657–663 (2007).

58. Olshen, A. B. *et al.* Parent-specific copy number in paired tumor-normal studies using circular binary segmentation. *Bioinformatics* **27**, 2038–2046 (2011).

59. Python Release Python 3.12.4. *Python.org* https://www.python.org/downloads/release/python-3124/.

60. Hunter, J. D. Matplotlib: A 2D Graphics Environment. *Computing in Science & Engineering* **9**, 90–95 (2007).

61. The pandas development team. pandas-dev/pandas: Pandas (v2.2.2). Zenodo https://doi.org/10.5281/zenodo.10957263 (2024).
62. Yu, G. enrichplot: Visualization of Functional Enrichment Result.
63. Wickham, H. *Ggplot2: Elegant Graphics for Data Analysis*. (Springer-Verlag, New York, 2016).
64. Mills, B. R. MetBrewer: Color Palettes Inspired by Works at the Metropolitan Museum of Art. (2022).
65. Arnold, J. B. *et al.* ggthemes: Extra Themes, Scales and Geoms for ‘ggplot2’. (2024).

Figure 1

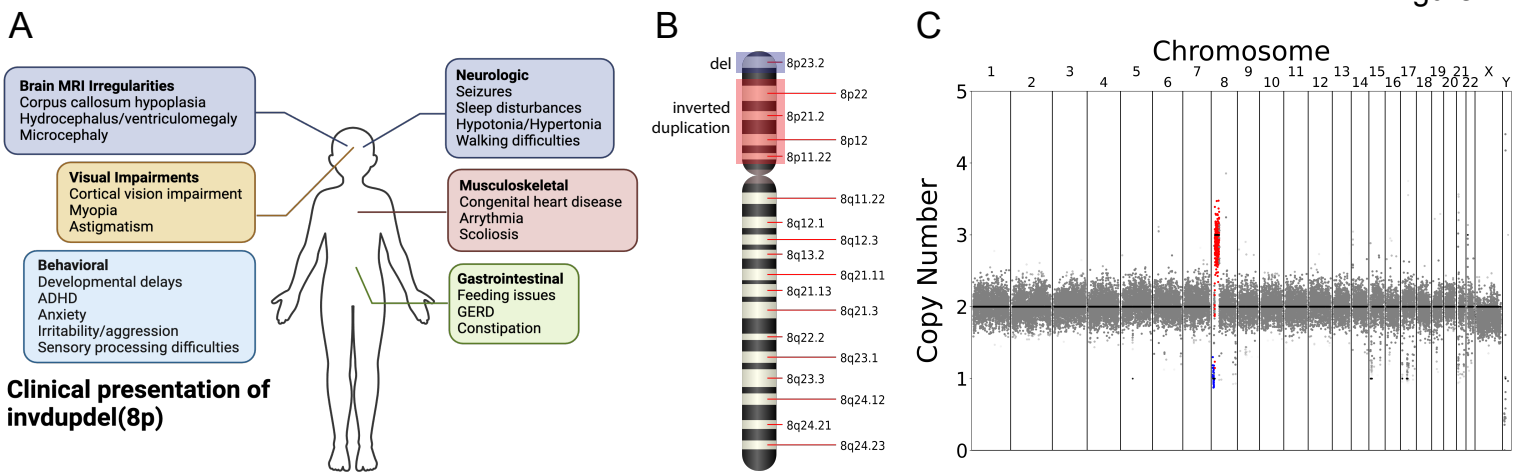
A
Brain MRI Irregularities
Corpus callosum hypoplasia
Hydrocephalus/ventriculomegaly
Microcephaly
Visual Impairments
Cortical vision impairment
Myopia
Astigmatism
Behavioral
Developmental delays
ADHD
Anxiety
Irritability/aggression
Sensory processing difficulties
Neurologic
Seizures
Sleep disturbances
Hypotonia/Hypertonia
Walking difficulties
Musculoskeletal
Congenital heart disease
Arrythmia
Scoliosis
Gastrointestinal
Feeding issues
GERD
Constipation
Clinical presentation of invdupdel(8p)
B
del
inverted duplication
8p23.2
8p22
8p21.2
8p12
8p11.22
8q11.22
8q12.1
8q12.3
8q13.2
8q21.11
8q21.13
8q21.3
8q22.2
8q23.1
8q23.3
8q24.12
8q24.21
8q24.23
C
Chromosome
1 2 3 4 5 6 7 8 9 10 11 12 13 14 15 16 17 18 19 20 21 22 X Y
Copy Number
0 1 2 3 4 5

Figure 2

A

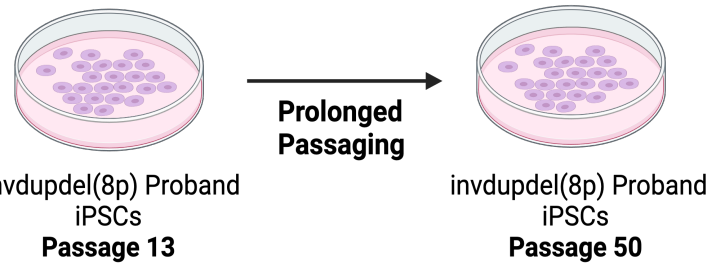
Prolonged Passaging
invdupdel(8p) Proband iPSCs
Passage 13
invdupdel(8p) Proband iPSCs
Passage 50

B

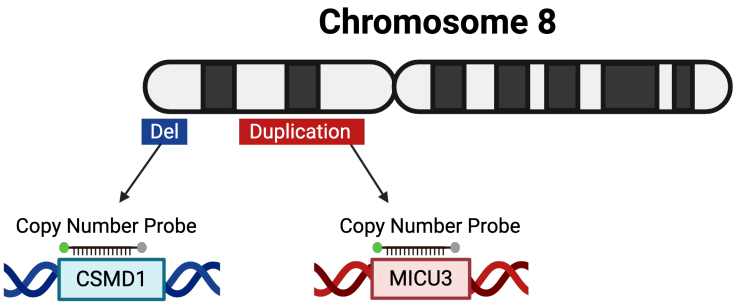
Chromosome 8
Del
Duplication
Copy Number Probe
CSMD1
Copy Number Probe
MICU3

C

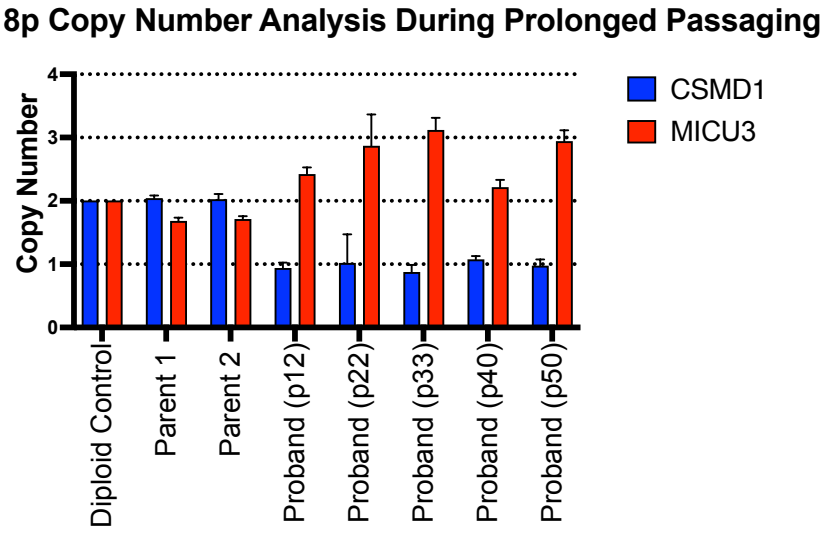
8p Copy Number Analysis During Prolonged Passaging
Copy Number
0
1
2
3
4
CSMD1
MICU3
Diploid Control
Parent 1
Parent 2
Proband (p12)
Proband (p22)
Proband (p33)
Proband (p40)
Proband (p50)

Figure 3

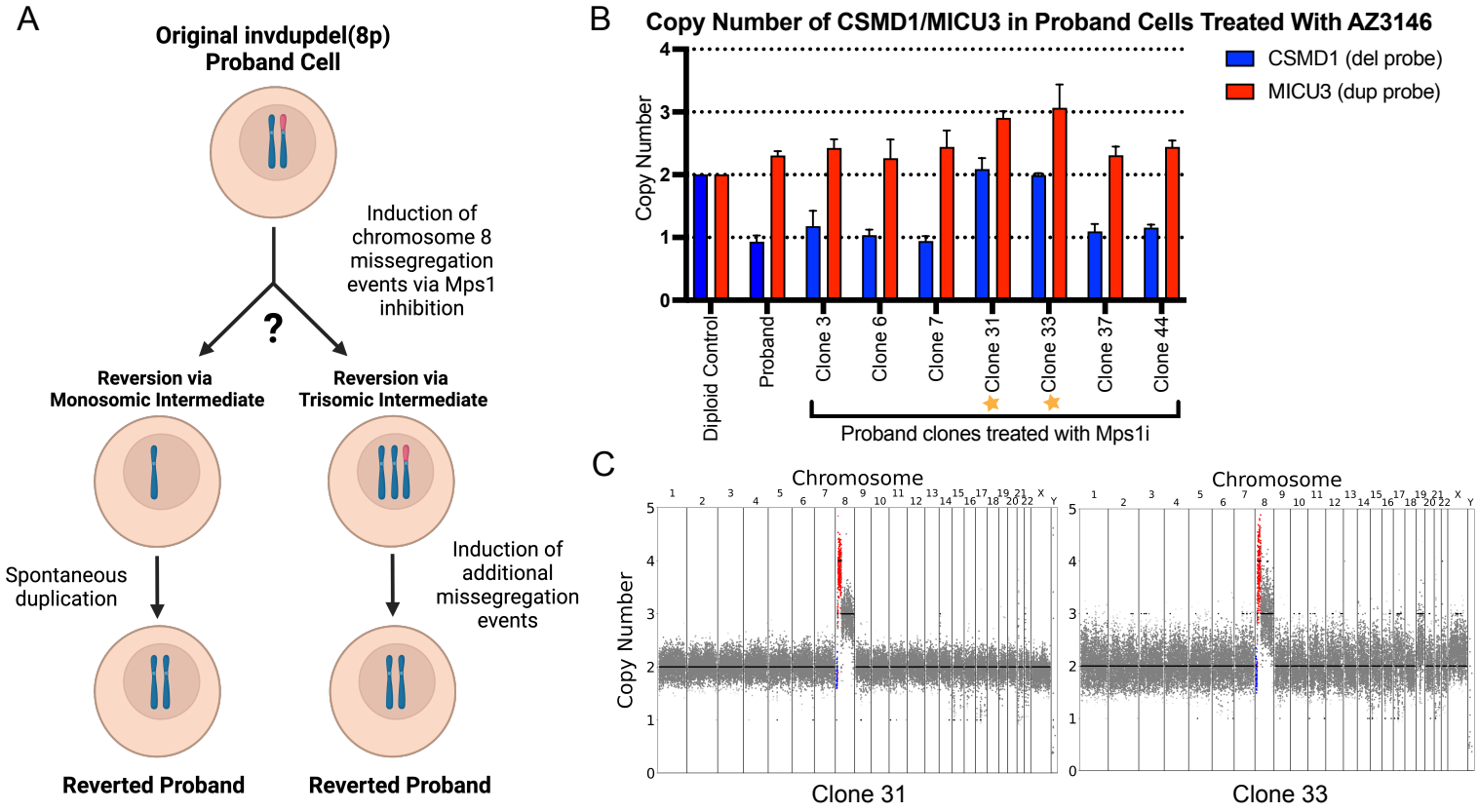
A
Original invdupdel(8p)
Proband Cell
Induction of chromosome 8 missegregation events via Mps1 inhibition
?
Reversion via Monosomic Intermediate
Reversion via Trisomic Intermediate
Spontaneous duplication
Induction of additional missegregation events
Reverted Proband
Reverted Proband
B
Copy Number of CSMD1/MICU3 in Proband Cells Treated With AZ3146
CSMD1 (del probe)
MICU3 (dup probe)
Copy Number
Diploid Control
Proband
Clone 3
Clone 6
Clone 7
Clone 31
Clone 33
Clone 37
Clone 44
Proband clones treated with Mps1i
C
Chromosome
Copy Number
Clone 31
Clone 33

Figure 4

A

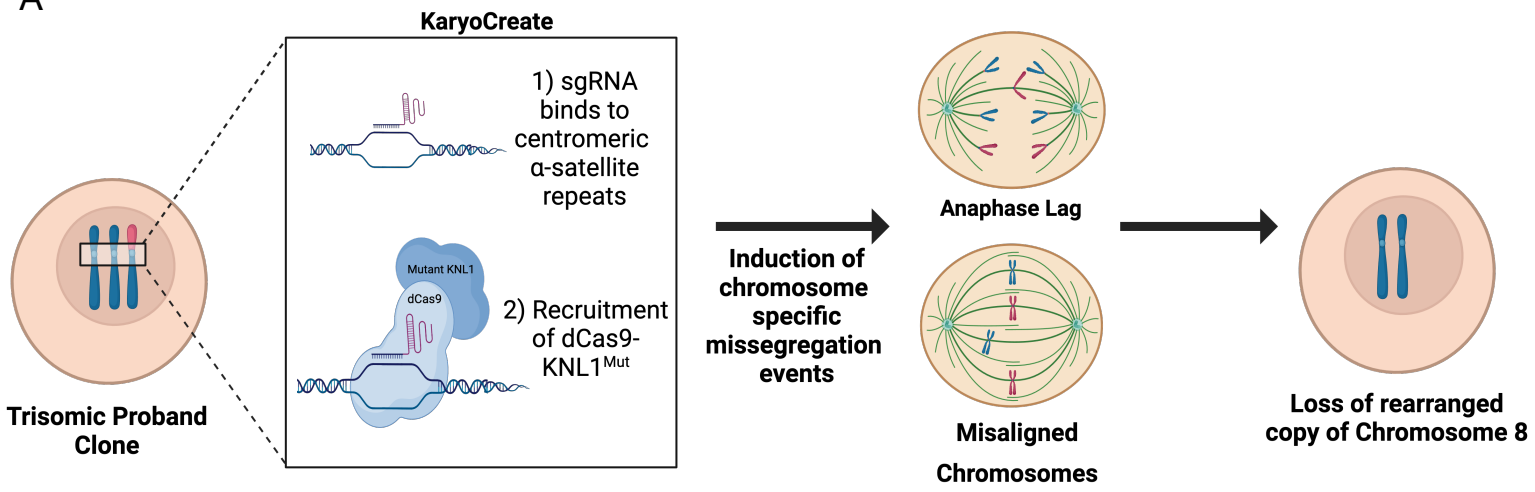
KaryoCreate
1) sgRNA binds to centromeric α-satellite repeats
Mutant KNL1
dCas9
2) Recruitment of dCas9-KNL1Mut
Trisomic Proband Clone
Induction of chromosome specific missegregation events
Anaphase Lag
Misaligned Chromosomes
Loss of rearranged copy of Chromosome 8

B

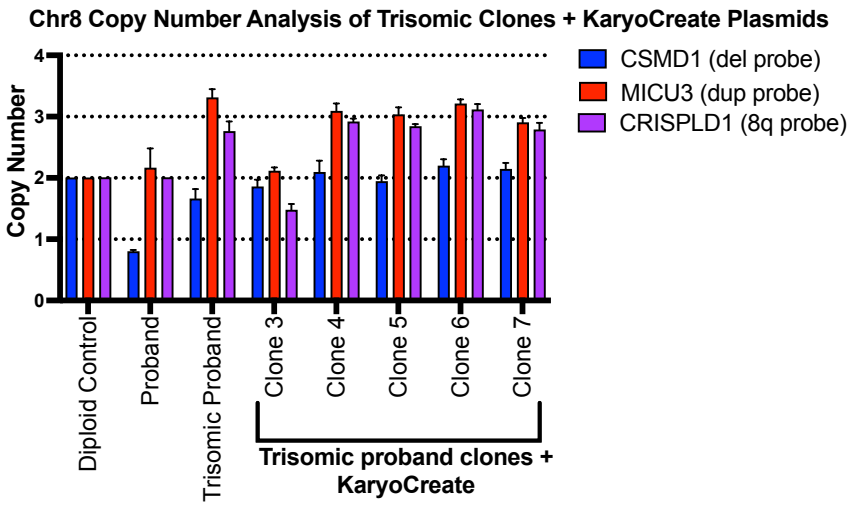
Chr8 Copy Number Analysis of Trisomic Clones + KaryoCreate Plasmids
CSMD1 (del probe)
MICU3 (dup probe)
CRISPLD1 (8q probe)
Copy Number
0
1
2
3
4
Diploid Control
Proband
Trisomic Proband
Clone 3
Clone 4
Clone 5
Clone 6
Clone 7
Trisomic proband clones + KaryoCreate

C

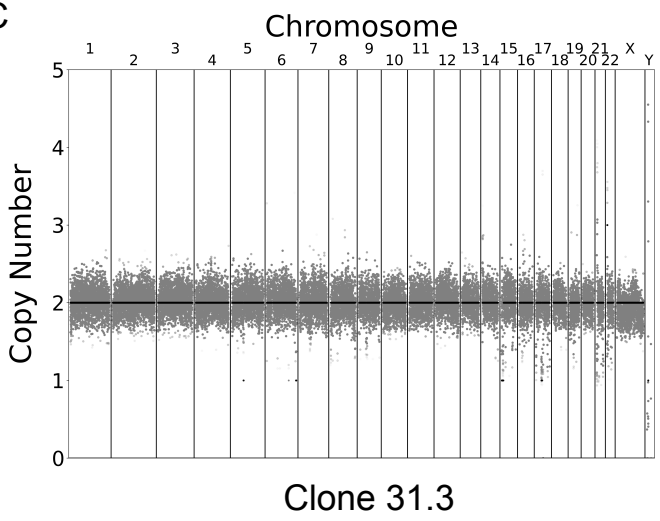
Chromosome
1 2 3 4 5 6 7 8 9 10 11 12 13 14 15 16 17 18 19 20 21 22 X Y
Copy Number
0
1
2
3
4
5
Clone 31.3

Figure 5

A

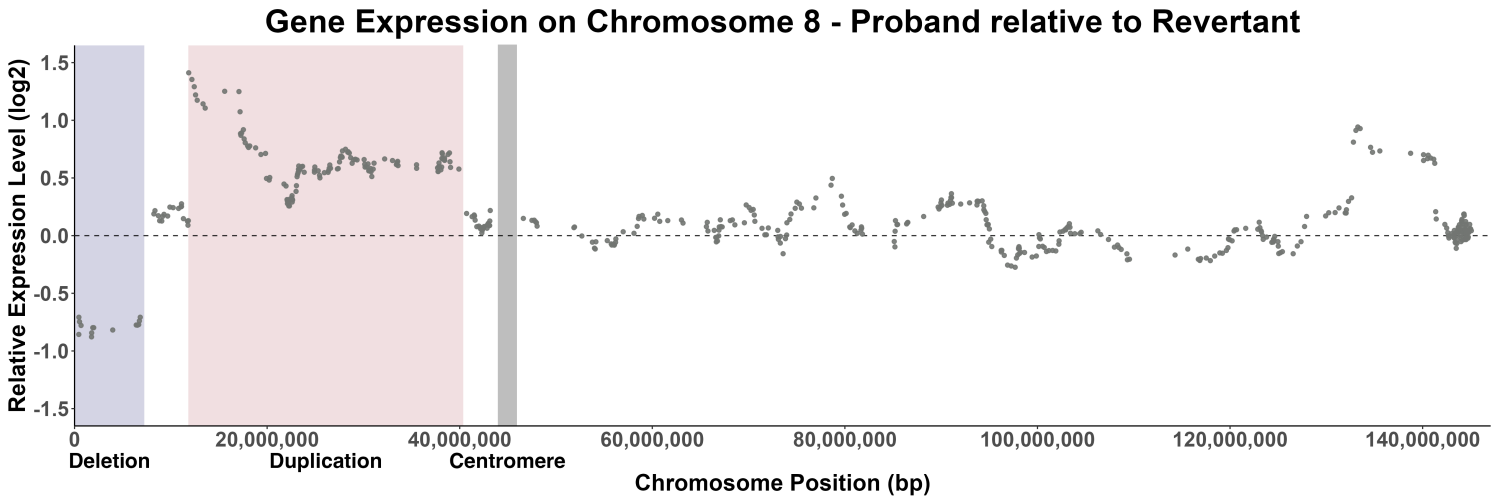

B

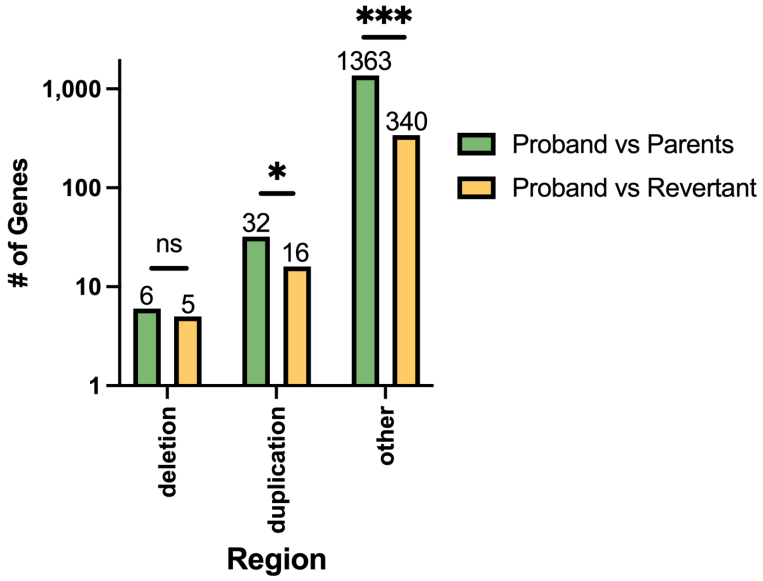

C

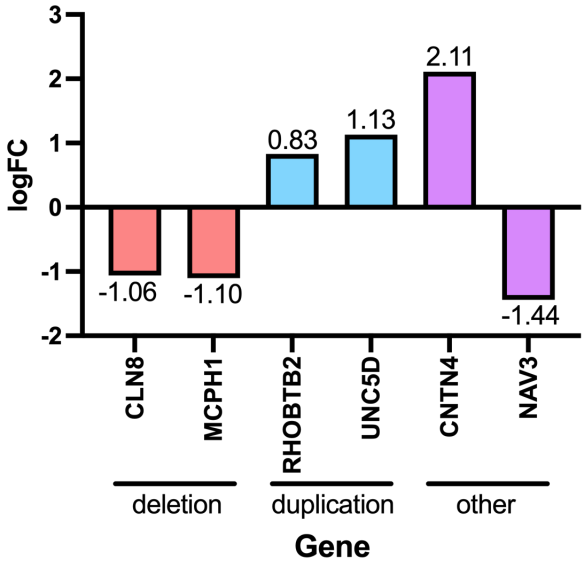

D

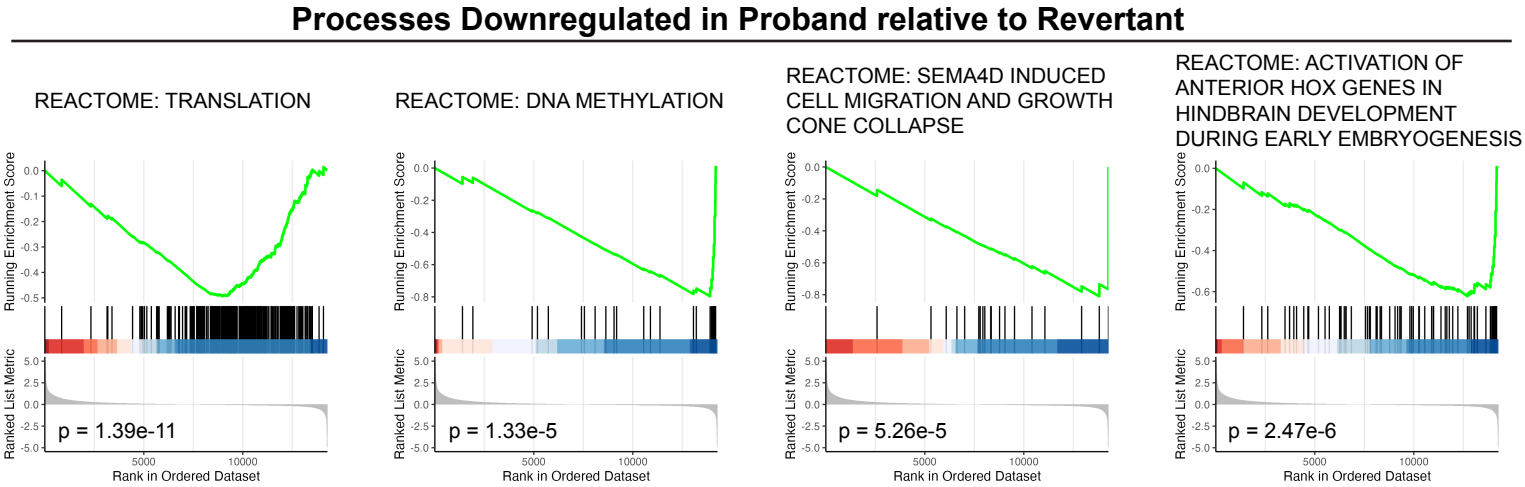

Figure S1

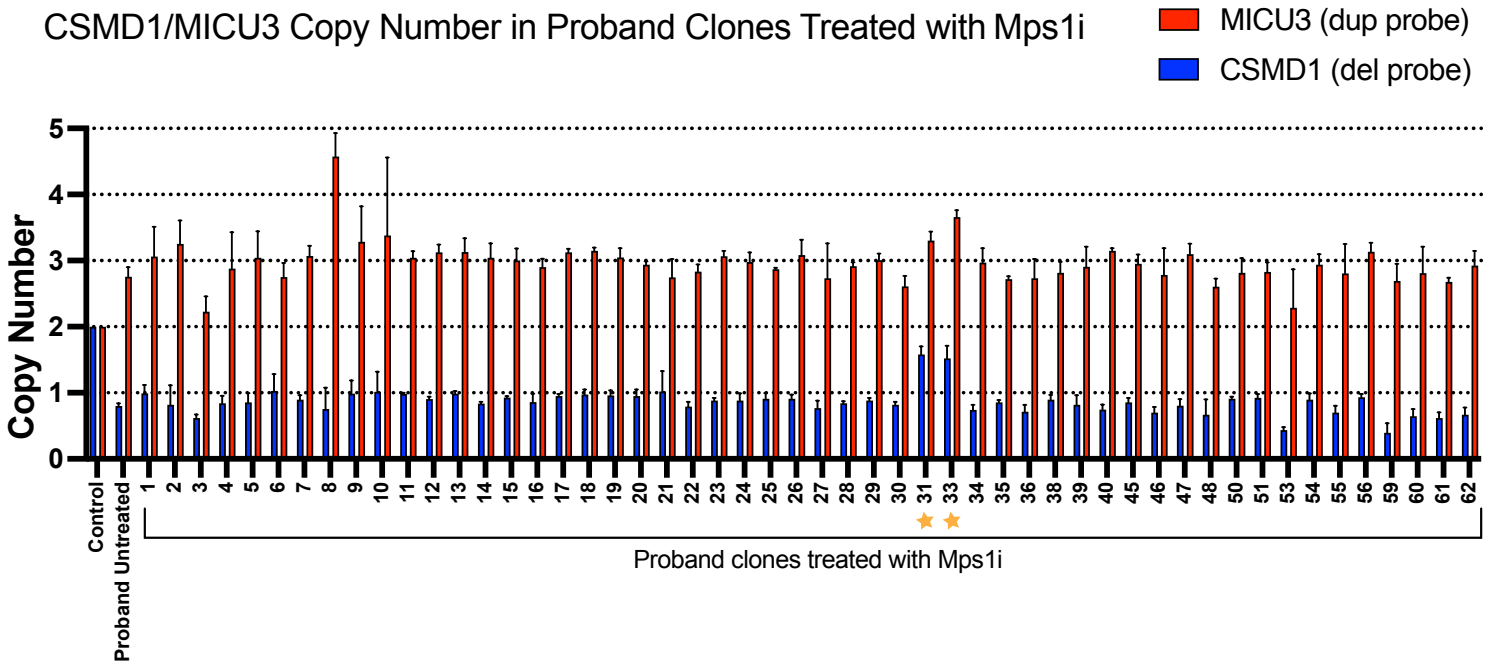
CSMD1/MICU3 Copy Number in Proband Clones Treated with Mps1i
MICU3 (dup probe)
CSMD1 (del probe)
Copy Number
0
1
2
3
4
5
Control
Proband Untreated
1 2 3 4 5 6 7 8 9 10 11 12 13 14 15 16 17 18 19 20 21 22 23 24 25 26 27 28 29 30 31 33 34 35 36 38 39 40 45 46 47 48 50 51 53 54 55 56 59 60 61 62
Proband clones treated with Mps1i

Figure S2

A

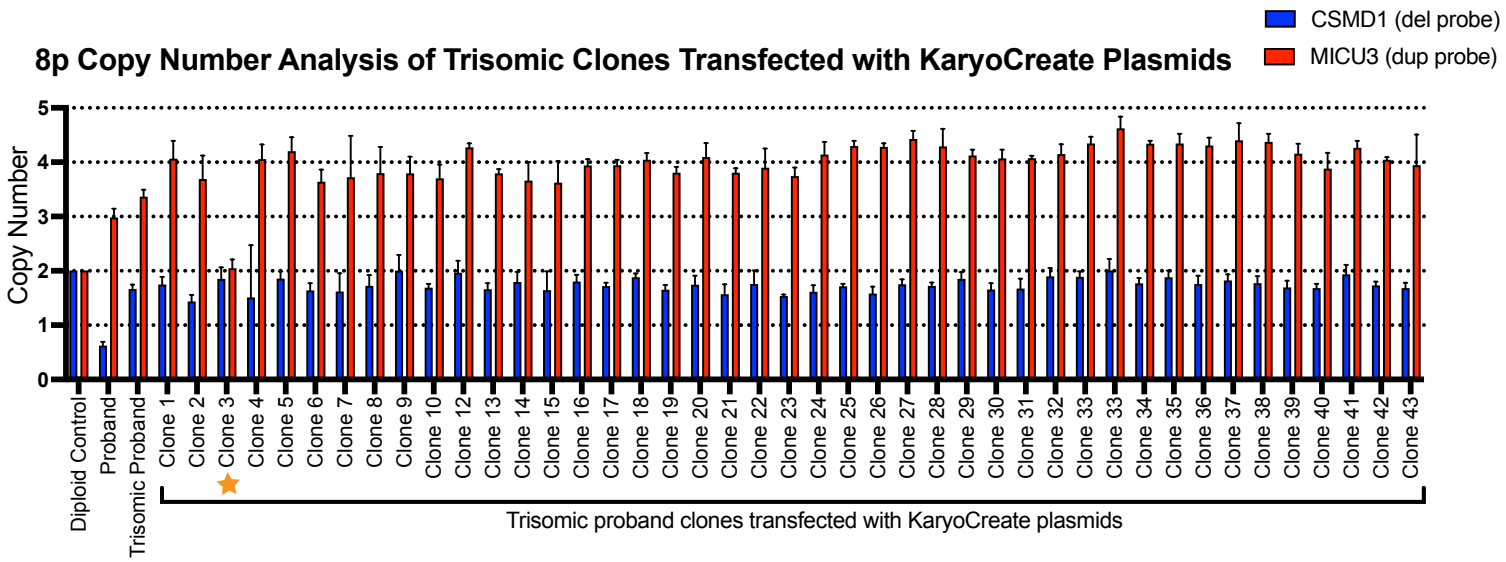

B

STR Profiles

Locus	Parent 1		Parent 2		Proband		Reverted Proband	
D5S818	12	12	11	11	11	12	11	12
D13S317	9	12	12	12	9	12	9	12
D7S820	10	10	8	9	9	10	9	10
D16S539	11	13	13	13	13	13	13	13
VWA	17	18	16	17	17	17	17	17
TH01	6	9.3	6	9	9	9.3	9	9.3
AM	X	X	X	Y	X	X	X	X
TPOX	8	11	11	11	11	11	11	11
CSF1PO	12	13	10	10	10	12	10	12
D3S1358	15	15	17	19.1	15	19.1	15	19
D21S11	29	33.2	28	29	28	29	28	29
D18S51	14	14	13	15	13	14	13	14
Penta_E	5	15	7	13	7	15	7	15
Penta_D	9	9	12	14	9	12	9	12
D8S1179	8	17	9	10	10	17	10	10
FGA	21	22	23	24	21	24	21	24